Original article

Simultaneous determination of bicyclol and its two active metabolites concentration in rat plasma and application for pharmacokinetics study of bicyclol and optimized bicyclol-nanoparticles

Xucong Huang [a,b,1], Zhenghua Wu [c,d,1], Yanchao Liu [c], Mengqi Jia [c], Wenjuan Zhao [d], Shuowen Wang [c,d], Xinhui Jiang [b,*], Yuefen Lou [a,*], Guorong Fan [b,c,d,*]

[a] Department of Pharmacy, Shanghai Fourth People's Hospital Affiliated to Tongji University School of Medicine, Shanghai 200434, PR China
[b] School of Pharmacy, Chongqing Medical University, Chongqing 400016, PR China
[c] Department of Clinical Pharmacy, Shanghai General Hospital, Shanghai Jiaotong University School of Medicine, Shanghai 200080, PR China
[d] School of Pharmacy, Shanghai Jiao Tong University, Shanghai 200240, PR China

ARTICLE INFO

ABSTRACT

A simple, sensitive, and rapid LC-MS/MS method for the simultaneous determination of BIC, the M7 and M8 active metabolites in SD rat plasma was developed. After salting-out assisted liquid–liquid extraction (SALLE) with 5 M ammonium acetate solution, the sample was analyzed on a Sciences column (C18 3.0 × 100 mm, 3 μm) using a gradient elution at 40 ℃ within 7 min. The assay displayed excellent linearity in the range of 4–2000 ng/mL for M7 and BIC, and 1–500 ng/mL for M8. The results of this method exhibited that the precision, accuracy, matrix effect, recovery, and stability of BIC, M7 and M8 met all requirements for the quantitation in plasma samples. The pharmacokinetic result showed that the $AUC_{(0 \to t)}$ was calculated as 383.1 ± 164.4 (ng/mL·h) for BIC, and 5627 ± 1261 (ng/mL·h) for M7 after oral administration with BIC. Compared with BIC group, the pharmacokinetic parameters in BIC-NPs group were improved. Augmentation in $AUC_{(0 \to t)}$ (3.02-fold) and $t_{1/2}$ (1.43-fold) for BIC. Meanwhile, double peak phenomenon was observed on the mean plasma concentration–time curves of M7 in BIC and BIC-NPs group. In conclusion, both BIC and BIC-NPs were metabolized to abundant M7 in SD rat, which would provide a basis for researching the treatment mechanism of liver injury.

© 2023 The Author(s). Published by Elsevier B.V. on behalf of King Saud University. This is an open access article under the CC BY-NC-ND license (http://creativecommons.org/licenses/by-nc-nd/4.0/).

1. Introduction

Bicyclol (BIC, methyl 5′-(hydroxymethyl)-7,7′-dimethoxy-[4,4′-bibenzo [d] [1,3] diox-ole]-5-carboxylate), a first-in-class hepatoprotectant, is based on derivative of traditional Chinese medicine (TCM) Schisandra chinensis (Wuweizi) of North(Hu et al., 2020). In 2004, Chinese Food and Drug Administration issued

the production license for BIC (Liu 2009). Nowadays, BIC has been widely used to treat liver injury and many researchers have illustrated that it possesses a variety of pharmacological activities (Zhao et al., 2021), including anti-viral effect (Ferenci 2015), anti-inflammatory(Zhao et al., 2020), anti-oxidative effects(Zhao et al., 2008), antisteatotic effects (Yu et al., 2009), anti-fibrotic effects(Zhen et al., 2015), and antitumor effects(Wang et al., 2016).

However, BIC has low bioavailability (9%), which is mostly a result from P-gp mediated efflux and metabolism by CYP3A in the intestine(Tan et al., 2008). When BIC was used to treat virus hepatitis or fatty liver disease, the cause of oral BIC was proposed to be 6 months at least(Yao et al., 2005, Tang et al., 2022). From our previous study(Huang et al., 2022), two active metabolites of BIC were identified and prepared, meanwhile, they possessed higher efficacy than BIC, which was verified by the isoniazid-induced liver injury zebrafish model(Huang et al., 2023). Therefore, it is of pivotal importance to monitor the metabolic profiles of BIC and the two active metabolites for pharmacodynamic evaluation. Meanwhile, BIC solubility is poor (0.04 mg/mL)(Tan et al., 2008), which

* Corresponding authors.
E-mail addresses: hxc1109060643@163.com (X. Huang), wuzhenghua526@163.com (Z. Wu), yanchaoliu0312@163.com (Y. Liu), jmq0701@163.com (M. Jia), zhaowj@sjtu.edu.cn (W. Zhao), wangshuowensy@163.com (S. Wang), jiangxinhui@cqmu.edu.cn (X. Jiang), louyuefen@sina.cn (Y. Lou), guorfan@163.com (G. Fan).
[1] These authors contributed equally to this paper.

Peer review under responsibility of King Saud University.

also limits BIC's clinical application. Jae Kuk Ryu(Ryu and Yoo 2012) prepared bicyclol microemulsions to enhance BIC's solubility and oral bioavailability. Whereas the security and efficacy of the BIC microemulsions need further evaluation. Therefore, we synthesized Bicyclol–Nanoparticles (BIC-NPs) by BIC and human serum albumin(Liu et al., 2022). The solubility of BIC was enhanced from 0.04 to 1 mg/mL. BIC-NPs security has been evaluated by AML-12 mouse hepatocytes cells and macrophages (RAW 264.7) and its efficacy has been verified by methotrexate induced-liver injury rat. However, the metabolism of BIC-NPs needs further investigation, which is useful for understanding its therapeutic mechanism. Thus, this study aimed to establish an effective and convenient method to simultaneously determine BIC, M7 and M8 in SD rat plasma for the pharmacokinetics study.

Since the composition of the biological sample is complex, sample pre-treatment must be conducted before LC-MS analysis (Ahmed et al., 2022). The three methods of protein precipitation (PPT), liquid–liquid extraction (LLE), and solid-phase-extraction (SPE) were widely used for sample pre-treatment(Li et al., 2021). However, PPT may cause high matrix effects with insufficient sample purification(Zhang et al., 2010). LLE can't extract target compounds invariably with the restriction of the low dielectric constant of extraction solvent(Pavan et al., 2022). SPE possesses high applicability on different samples but is complicated, time-consuming, and cost ineffective(Rizzo et al., 2020). Salting-out assisted liquid/liquid extraction (SALLE) with water-miscible organic solvent has shown its distinctive advantages in bioanalytical research(Anthemidis and Ioannou 2009, Tang and Weng 2013, Hajkova et al., 2016). The extraction solvent of SALLE can be polar solvent with high dielectric and abundant hydrogen donor which make up for the deficiency of LLE(Anthemidis and Ioannou 2009, Zhang et al., 2009).

In the current study, the metabolism of BIC-NPs in SD rat plasma was clarified and an effective LC-MS/MS method was established, verified, and subsequently applied to analyze the multicomponent pharmacokinetics of BIC, M7, and M8 in SD rat plasma following oral administration with BIC or BIC-NPs, or intravenous injection with BIC-NPs.

2. Material and method

2.1. Chemicals and materials

BIC was purchased from the Beijing Concorde pharmaceutical factory (batch no. 170657, purity 98.0%). Dimethyl dicarboxylate biphenyl (DDB; purity > 98%) was provided by Dalian Meilun Biotech Co., Ltd. M7, M8 was prepared by our laboratory. Ammonium formate, formic acid and ammonium acetate were acquired from ANPEL Lab Tech. (Shanghai, China). Methotrexate (MTX), sodium dodecyl sulfate (SDS), dithiothreitol (DTT), human serum albumin (HSA), 4-morpholineethanesulfonic acid (MES), and urea were purchased from Aladdin Chemistry Co. Ltd.; The pure water (18.2 MΩ/ cm) was deionized by a Milli-Q system (Millipore, Bedford, MA, USA). Methanol and acetonitrile (LC/MS grade) were purchased

from Thermo Fisher Scientific China Co., Ltd. Methanol (LC grade) was acquired from Merck (Darmstadt, Germany).

2.2. UPLC-Q-TOF/MS instruments and conditions

Samples were analyzed on an Agilent 1290 Infinity UPLC system (Milford, MA, USA) equipped with an Agilent UPLC column (Poroshell 120 EC-C18 2.1 × 150 mm, 1.9 μm). The mobile phases consisted of (A) 0.1% formic acid and 2 mM ammonium formate aqueous solution and (B) acetonitrile. The gradient elution was optimized as follows: 0–12 min, 10%-30% B;12–15 min, 30%-60% B; 15–16 min, 60%-90% B; 16–17 min, 90% B; 17–18 min, 90%-10% B, post time 2 min. The flow rate was 0.3 mL/min. The column temperature was 45 ℃. The injection volume was 2 μL.

Mass spectrometric data were obtained by Agilent 6545 Q-TOF MS/MS equipped with a Dual Agilent Jet Stream electrospray ionization (ESI) source. The ESI source was set in positive ionization mode. The parameters in the source were set as follows: scan range, 100–1000 *m/z* (MS) and 50–800 *m/z* (MS/MS); fragmentor voltage, 175 V; gas temperature, 320 ℃; sheath gas temperature, 350 ℃; sheath gas flow, 11 L/min; and drawing gas flow, 8 L/ min; nebulizer gas pressure, 35 psig. the collision energy was operated at alternative voltages of 10–30 eV.

2.3. LC-MS/MS instruments and conditions

Samples were analyzed on an Agilent 1260 Infinity HPLC system (Milford, MA, USA) equipped with a Sciences column (C18 3.0 × 1 00 mm, 3 μm). The mobile phases consisted of (A) 0.1% formic acid and 4 mM ammonium formate aqueous solution and (B) acetonitrile. The gradient elution was optimized as follows: 0–3 min, 30%-50% B; 3–3.1 min, 40%-95% B; 3.1–5 min, 95% B; 5–5.1 min, 95% −30%B; 5.1–7 min, 30%B, post time 2 min. The flow rate was 0.5 mL/min. The column temperature was 40 ℃. The injection volume was 2 μL.

Mass spectrometric data were obtained by Agilent G6400 LC-MS/MS system equipped with a Dual Agilent Jet Stream electrospray ionization (ESI) source. The ESI source was set in positive ionization mode. The parameters in the source were set as follows: gas temperature, 325 ℃; sheath gas temperature, 400 ℃; sheath gas flow, 11 L/min; and gas flow, 8 L/min; nebulizer gas pressure, 40 psig. BIC enantiomers and the two active metabolites were quantified by Multiple reaction monitoring (MRM). The compound-dependent parameters of the four MRM channels including cell accelerator voltage (CAV), collision energy (CE), and fragmentor (FM), were optimized individually by MassHunter Optimizer and were displayed in Table 1. Agilent MassHunter Workstation® (version B.08.03, Agilent Technologies Inc., Santa Clara, CA, USA) was used for system control, data acquisition, fragment optimizer, and data processing.

2.4. Preparation of calibration standards and quality control (QC) samples

The BIC, DDB, the M7 and M8 were accurately weighed and dissolved in ACN to yield stock solutions with a concentration of

Table 1
Optimized mass spectrometry conditions for BIC, M7 and M8.

Analytes	Precursor Ion (Da)	Product Ion (Da)	FM (V)	CE (V)	CAV (V)
Bicyclol	373.0	387.0	109.0	12.0	4.0
Bifendate	419.0	341.0	82.0	4.0	4.0
M7	361.0	329.0	103.0	8.0	4.0
M8	359.0	327.0	108.0	8.0	4.0

Note: CAV, cell accelerator voltage; CE, collision energy; FM, fragmentor.

1 mg/mL. Working standard solutions were diluted from the stock solutions with an ACN: H₂O (50:50) mixture. The final concentrations range of working standard solutions of BIC, and M7 were 40–20,000 ng/mL, and M8 was 10-5,000 ng/mL.

Samples for the calibration curve and QC were prepared by SALLE. The final calibration standards were 4, 20, 40, 200, 400, 1000, 2000 ng/mL for BIC and M7, and 1, 5, 10, 50, 100, 250, 500 ng/mL for M8. The concentrations of QC samples at low, medium, and high levels were 10, 100, and 1600 ng/mL for BIC and M7, and 2.5, 25, and 400 ng/mL for M8.

2.5. Sample preparation

Two different sample preparation methods, SALLE and PPT, were compared in this study.

PPT method: 90 μL blank plasma, 10 μL working standard solution (1 μg/mL), and 10 μL IS (2 μg/mL) were successively added into 1.5 mL Eppendorf (EP) tube and the mixture was vortexed for 30 s. Next, 200 μL of 100% acetonitrile was added for protein precipitation followed by vortex (3 min) and centrifugation (12,000 rpm, 10 min), and the supernatant was finally collected and 2 μL was used for LC–MS/MS analysis.

SALLE method: 90 μL blank plasma, 10 μL working standard solution (1 μg/mL), 10 μL IS (2 μg/mL), and 100 μL 5 M ammonium acetate solution were successively added into 1.5 mL Eppendorf (EP) tube and the mixture was vortexed for 30 s. The subsequent steps were the same as PPT.

2.6. Tested LC-MS/MS method validation

The validation procedures were performed based on international recommendations published by FDA.

2.6.1. Specificity and selectivity

The specificity and selectivity of the method for each validation series was proved using 6 individual sources of blank plasma. The peak area at the retention time of the analyte in blank samples should be <20% of LLOQ and <5% for the IS.

2.6.2. Residual effects

Residual effect was evaluated by injecting a blank plasma sample after the highest CAL. The eluting peaks area of the blank plasma at the retention times of each analyte should <20% of the LLOQ and 5% of the IS peak area.

2.6.3. Linearity and sensitivity

The linearity ranges of BIC, M7, and M8 were chosen from our preliminary experiment. For each linearity range, the response of highest point were more than three times as much as the actual blood sample after 6 h of oral administration with BIC-NPs. The calibration curves contained seven points and were generated using a $1/x^2$ weighted linear least-squares regression. The degree of fitness calculated using correlation coefficient (r) had to be > 0.990. The accuracy of each concentration point had to be in the range of 85%–115%, except for lower limit of quantification (LLOQ), which had to be in the range of 80%–120%.

2.6.4. Accuracy and precision

For determining the accuracy and precision, LLOQ and three different concentrations of QCs (low, medium, high) samples from the same day were analyzed with three consecutive days (n = 6). Relative recovery (RR) was used to define the accuracy. Relative Standard Deviation (RSD) was used to calculate the intra and inter-batch precisions. The RR had to be in the range of 85%–115% (80%–120% for LLOQ), and the RSD had to be <±15% (±20% for LLOQ).

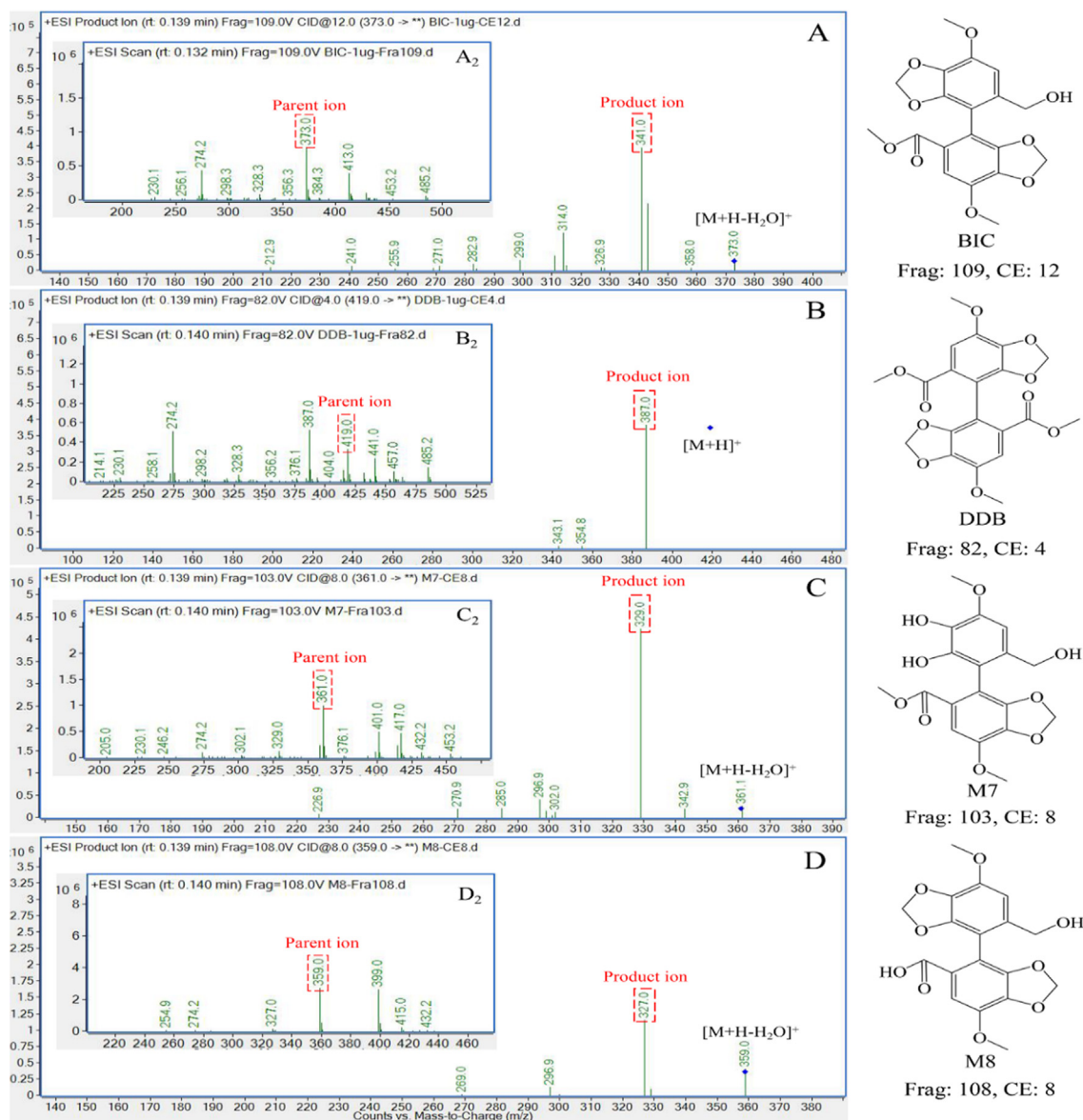#### 2.6.5. Extraction recovery and matrix effect

Three different sample sets were prepared: (1) stock solutions containing all the compound and IS were diluted by pure water; (2) Three different concentrations of QCs. (3) stock solutions containing all the compounds and IS were added into pretreatment blank plasma. The final concentration of the three groups was the same. The extraction recovery of each compound was evaluated as the peak area ratio of (2) to (3). The matrix effect of each compound was evaluated as the peak area ratio of (3) to (1). The extraction recovery and matrix effects had to be in the range of 80–120%.

2.6.6. Dilution effect

Dilution integrity was investigated using drug free plasma spiked at 2-fold of high QC in six replicates, dilution folds (1:2 and 1:4). The RR should be within 85% to 115%, and the RSD should be within ± 15%. Diluted samples were then treated as under described in Section 2.5.

2.6.7. Stability

The stability of all compounds in plasma was studied by analyzing the three QCs in different conditions (n = 6). (1) The prepared sample was placed in the autosampler 12 h before injection. (2) The unextracted sample was placed in room temperature (RT) 6 h before sample preparation and analysis. (3) The unextracted

Table 2
The ms/ms data of bic-nps and metabolites.

NO.	Formular	RT(min)	[M + H-H₂O]⁺			Fragment ions
			m/z	Calc m/z	Diff (ppm)	
M1	$C_{24}H_{24}O_{15}$	6.10	535.1094	535.1088	1.12	359.0757, 327.0497, 297.0391
M2	$C_{24}H_{24}O_{15}$	6.57	535.1073	535.1088	−2.80	359.0757, 327.0495, 297.0389
M4	$C_{25}H_{26}O_{15}$	8.01	566.4273	566.4295	−3.88	390.0845, 358.0637, 328.0519
M5	$C_{18}H_{18}O_{9}$	8.39	361.0906	361.0923	−4.71	329.0642, 297.0387, 269.0435
M6	$C_{24}H_{24}O_{15}$	8.61	535.1081	535.1088	−1.31	359.0753, 327.0486, 297.0385
M7	$C_{18}H_{18}O_{9}$	9.91	361.0917	361.0923	−1.66	329.0657, 297.0386, 269.0435
M8	$C_{18}H_{16}O_{9}$	11.30	359.0760	359.0766	−1.67	327.0502, 297.0394, 269.0442
M9	$C_{19}H_{18}O_{9}$	11.36	373.0923	373.0920	0.80	343.0805, 341.0652, 314.0777
M10	$C_{18}H_{16}O_{9}$	12.06	359.0762	359.0766	−1.11	329.0653, 327.0500, 300.0629
M11	$C_{19}H_{20}O_{9}$	13.19	375.1076	375.1080	−1.07	343.0784, 331.1286, 313.1151
			[M + H]⁺			
			m/z	Calc m/z	Diff (ppm)	
M3	$C_{18}H_{16}O_{8}$	6.85	361.0914	361.0923	−0.83	329.0656, 314.0419, 301.0695

Fig. 1. Parent ions scan (image shown inside the box) and products ions MRM spectra of (A) BIC, (B) DDB, (C) M7, (D) M8.

sample were placed in −40 ℃ 30 days before sample preparation and analysis. (4) The unextracted sample underwent three freeze–thaw cycles at room temperature or −40 ℃.

2.7. Synthesis of BIC-NPs

The synthesis method was from our previous study (Liu et al., 2022). First, a solution of 2% SDS and 0.15% DTT was used to eliminate hydrophobic forces and intramolecular disulfide bonds from SA. Then, the HSA solution was heated to 90 °C for 2 h to liberate free thiol groups, and BIC (in 1.0 mL of MES, 0.1 M, pH 4.8, stirred at 70 °C for 3 min) was spiked into the HSA solution and magnetically stirred at 770 rpm. Next, the reaction bottle was immersed in an ice bath. Following the thermal drive, molecular HSA was reformed into large-sized nanostructures via the reconstructed intermolecular disulfide bond and hydrophobic interaction. The abundance of binding sites between BIC and HSA nanostructures allowed for efficient BIC loading and NP formation. The treated HSA was redissolved in MES, and BIC-NPs were prepared by adding

different mass ratios of BIC in the reaction solution (BIC: HSA = 1: 2, 1: 5, 1: 7.5, and 1: 10; w/w).

2.8. Application of the method to pharmacokinetics of BIC and BIC-NPs in rats

15 Pathogen free male SD rats (180–200 g, 4–5 weeks) were provided by Shanghai Jiao Tong University. Rats were adaptively grown in the laboratory for a week before the experiment. 15 rats were randomly divided into three groups and each group was given drug once a day and lasting five days: group Ⅰ was orally administrated with BIC (suspended in 0.5% carboxymethyl cellulose, 1 mg/mL) 15 mg/kg; groupⅡ was administrated with BIC-NPs (contains BIC 1 mg/mL) 15 mg/kg; group Ⅲ was intravenously injected with BIC-NPs (contains BIC 1 mg/mL) 1.5 mg/kg. The blank blood samples were collected before oral administration. The blood samples were collected into heparinized tubes at 5 min, 15 min, 30 min, 45 min, 1 h, 2 h, 3 h, 6 h, 12 h, and 24 h after the fifth day oral administration or intravenous injection and immediately
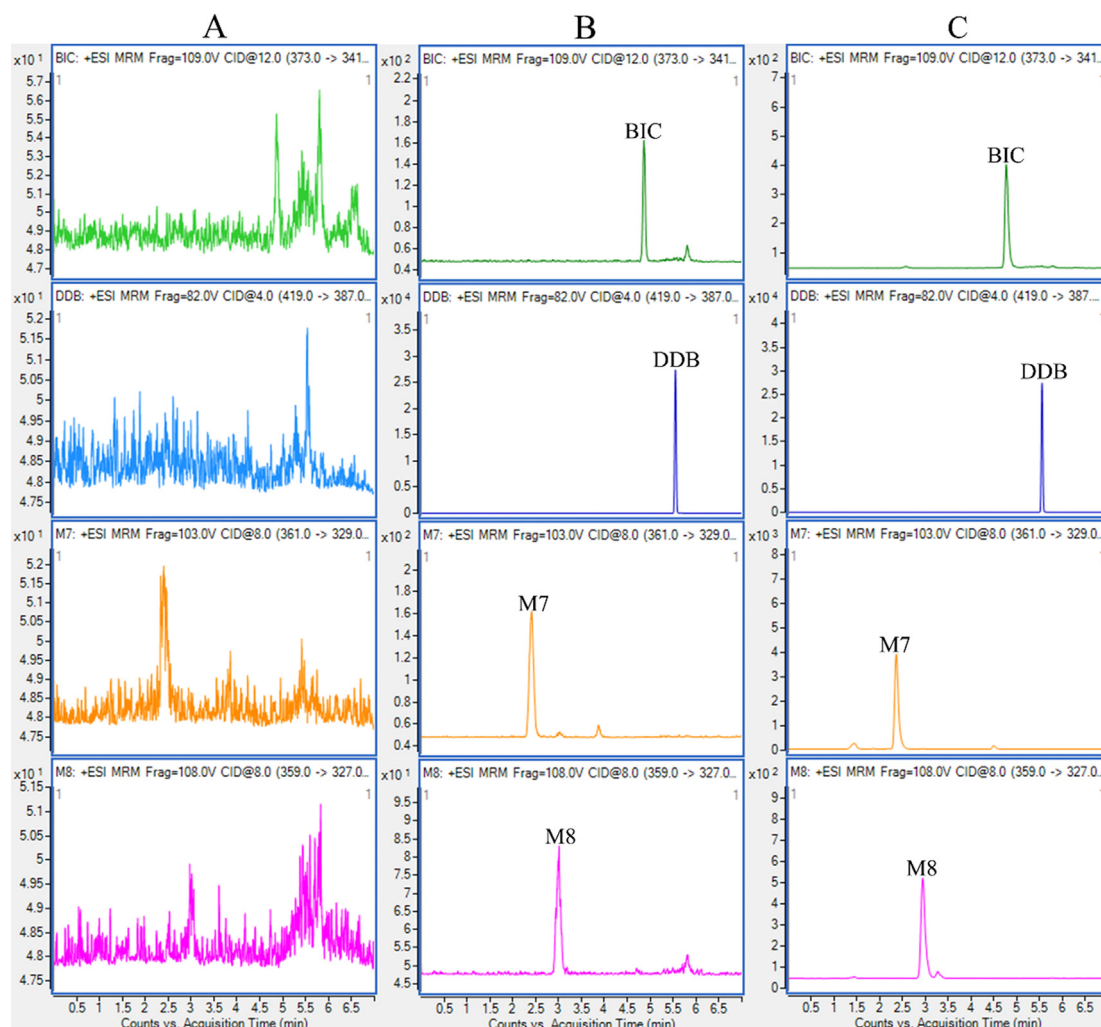
Fig. 2. Representative MRM chromatograms of BIC, M7, M8, and IS in SD rat sample: blank plasma (A), LLOQ for each analyte (B) and rat blood sample after 6 h of orally administrated with BIC-NPs (C).

Table 3
The regression equations, linear range and LLOQs of BIC, M7, and M8.

Analyte	Regression equation	r	Linear range (ng/mL)	LLOQ (ng/mL)
BIC	Y = 0.189X + 0.0038	0.996	4–2000	4
M7	Y = 0.152X + 0.0012	0.998	4–2000	4
M8	Y = 0.206X + 0.0011	0.993	1–500	1

placed in ice. Collection tubes were gently inverted for 4–5 times and centrifuged at 3000 rpm for 5 min at 4 ℃. The separated plasma samples were collected and stored at −80 ℃ until analysis.

Animal studies were performed following the recommendations in the Guidelines for the Care and Use of Laboratory Animals and relevant Chinese laws and regulations, which were approved by the Institutional Animal Care and the Use Committee of Shanghai Jiao Tong University (approval number A2018075).

3. Results and discussion

3.1. Identification of BIC-NPs metabolites in SD rat plasma

Firstly, the metabolite identification was conducted on UPLC-Q-TOF-MS/MS to investigate whether the metabolites of optimized BIC-NPs were changed in SD rat plasma. The analyzed plasma sample was prepared from the rats after 1, 2, and 6 h after oral administration with BIC-NPs. 11 metabolites of BIC-NPs were tentatively identified and are listed in Table 2. The relative mass spectrums are shown in Fig. S1. The proposed metabolic pathways of BIC-NPs in SD rat plasma are shown in Figure S2. Compared with BIC the main metabolites of BIC-NPs were not changed(Huang et al., 2022). Consequently, the active M7 and M8 metabolites possess superior pharmacodynamics than BIC which was verified on the isoniazid (INH)-induced liver injury zebrafish model and were chosen for quantitative analysis(Huang et al., 2023).

3.2. LC-MS/MS condition optimization

The optimization of LC-MS/MS condition were conducted on the mobile phase, the compound-dependent parameters, and the gradient elution. As only [M + Na]⁺ ions was detected for BIC, M7,

Table 4
Accuracy and precision of intra- and inter-batch at lower limit of quantification, low, medium, and high concentrations.

Analytes	Spiked Conc.(ng/mL)	Intra-batch (n = 6)			Inter-batch (n = 18)		
		Mean ± SD conc.(ng/mL)	Precision (%RSD)	Accuracy (%RR)	Mean ± SD conc.(ng/mL)	Precision (%RSD)	Accuracy (%RR)
M7	4	4.08 ± 0.35	8.65	101.89 ± 8.82	3.89 ± 0.32	8.21	97.17 ± 7.98
	10	9.18 ± 0.63	6.82	91.85 ± 6.26	9.16 ± 0.46	4.97	91.65 ± 4.55
	100	93.98 ± 8.19	8.72	93.98 ± 8.19	92.74 ± 7.75	8.36	92.74 ± 7.75
	1600	1482 ± 106	7.20	92.63 ± 6.67	1502 ± 106	7.09	93.88 ± 6.66
M8	1	0.95 ± 0.11	11.16	94.76 ± 10.57	0.97 ± 0.11	11.06	97.41 ± 10.78
	2.5	2.32 ± 0.16	6.71	92.66 ± 6.22	2.30 ± 0.12	5.38	92.18 ± 4.96
	25	23.69 ± 1.83	7.71	94.78 ± 7.31	23.21 ± 1.58	6.82	92.83 ± 6.33
	400	377.8 ± 31.4	8.33	94.46 ± 7.87	387.31 ± 31.08	8.03	96.83 ± 7.77
BIC	4	3.92 ± 0.30	7.62	98.07 ± 7.48	4.18 ± 0.33	7.99	104.61 ± 8.36
	10	9.59 ± 0.66	6.85	95.86 ± 6.57	9.72 ± 0.76	7.78	97.17 ± 7.56
	100	97.92 ± 7.66	7.82	97.92 ± 7.66	94.56 ± 5.89	6.23	94.56 ± 5.89
	1600	1473 ± 85.7	5.82	92.09 ± 5.36	1535 ± 118	7.71	95.95 ± 7.40

Note. Conc. Concentration;

Table 5
Matrix effects and recoveries of BIC, the M7, M8 metabolite and DDB.

Analytes	Concentration (ng/mL)	Matrix Effect (%)		Recovery	
		Mean ± SD	RSD (%)	Mean ± SD	RSD (%)
M7	10	93.35 ± 5.82	6.23	90.69 ± 3.59	3.96
	100	90.35 ± 4.43	4.91	92.93 ± 4.07	4.38
	1600	93.78 ± 6.24	6.65	90.77 ± 4.79	5.28
M8	2.5	96.63 ± 4.52	4.68	92.30 ± 2.62	2.84
	25	95.35 ± 2.85	2.99	102.95 ± 2.84	2.76
	400	96.18 ± 2.26	2.35	90.12 ± 3.00	3.33
BIC	10	93.12 ± 5.65	6.07	87.85 ± 4.22	4.81
	100	97.76 ± 2.82	2.88	87.59 ± 5.11	5.11
DDB	1600	94.80 ± 3.67	3.87	96.42 ± 4.48	4.65
	100	93.65 ± 2.46	2.63	96.94 ± 1.67	1.72

Table 6
Stability of analytes in different storage conditions (n = 6 for each value).

| Ana-lytes	Spiked Conc.(ng/mL)	RT Stability		Autosampler Stability		Freeze-Thaw Stability		Long-Term Stability	
		Accuracy (%RR)	Precision (%RSD)	Accuracy (%RR)	Precision (%RSD)	Accuracy (%RR)	Precision (%RSD)	Accuracy (%RR)	Precision (%RSD)
M7	10	102.61 ± 4.97	4.85	91.36 ± 2.63	2.87	92.63 ± 3.98	4.30	92.99 ± 4.85	5.22
	100	92.57 ± 4.14	4.47	98.25 ± 6.94	7.06	94.55 ± 5.35	5.65	91.73 ± 3.57	3.90
	1600	93.13 ± 5.89	6.32	93.90 ± 3.77	4.01	104.07 ± 6.83	6.56	93.50 ± 4.70	5.03
M8	2.5	92.67 ± 5.34	5.76	91.69 ± 7.38	8.05	102.27 ± 7.90	7.73	94.44 ± 7.32	7.75
	25	91.76 ± 5.79	6.31	100.22 ± 7.95	7.94	91.74 ± 4.01	4.37	94.67 ± 6.98	7.37
	400	95.65 ± 3.96	4.14	96.56 ± 7.40	7.66	94.13 ± 5.47	5.81	94.75 ± 4.68	4.94
BIC	10	101.14 ± 6.10	6.04	94.02 ± 6.55	6.97	102.47 ± 8.96	8.75	102.77 ± 7.87	7.66
	100	92.79 ± 3.85	4.15	93.52 ± 3.25	3.48	94.66 ± 3.79	4.01	91.53 ± 4.01	4.38
	1600	95.53 ± 6.37	6.67	93.92 ± 6.07	6.46	92.90 ± 5.79	6.23	95.91 ± 6.67	6.95

Note. Conc. Concentration; RT. Room Temperature.

and M8 with the mobile phase of 0.1%FA H_2O and ACN, ammonium formate was added to the water to generated $[M + H-H_2O]^+$ ions which were stable. In addition, 2 mM, 4 mM, 6 mM ammonium formate were tested, and the 4 mM ammonium formate was finally chosen for the best response and peak shapes. The compound-dependent parameters of the four MRM channels including CAV, CE, FM, were optimized individually by MassHunter Optimizer and were displayed in Table 1. The mass spectrograms of parent and product ions are shown in Fig. 1. DDB was chosen as internal standard for similar structure with BIC and non-interfering. As the isomeride M10 also was detected in the optimized MRM channel of M8, the elution gradient of 30%–50% ACN during 0–3 min

was added to separate M8 and M9. Furthermore, the organic phase ratio was enhanced to 95% to adequately clean the column. Finally, the elution gradient was optimized to 7 min for each analysis.

3.3. Sample preparation

The four methods of PPT, LLE, SALLE, and SPE were widely used for sample pre-treatment. As SPE is cumbersome and costly and LLE was restricted by the extraction solvent, PPT and SALLE was compared in this study. As shown in Fig. S3, the sample which was prepared by SALLE possessed lower endogenous impurity than that by PPT on the ultraviolet spectrogram at 276 nm. Meanwhile,
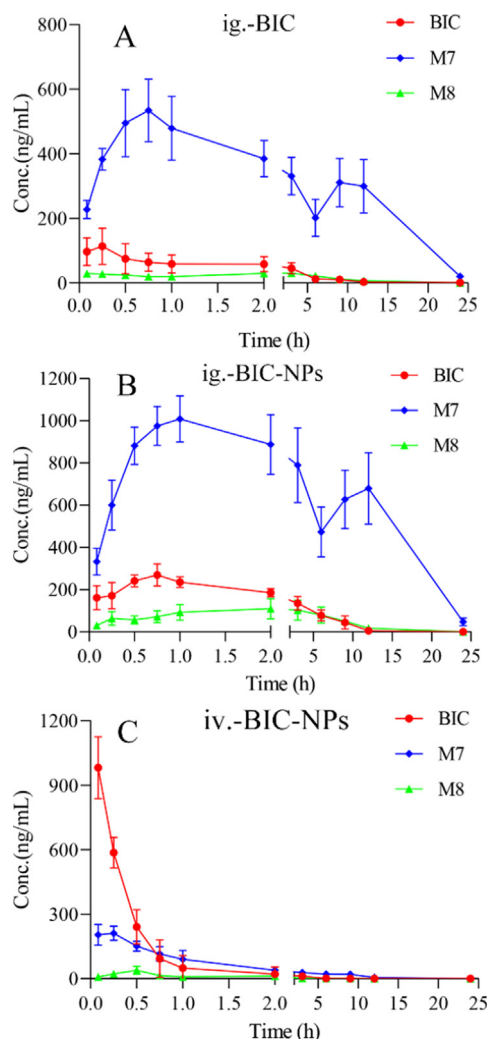
Fig. 3. The mean plasma concentration–time curves of BIC, M7, and M8 in SD rats (n = 5). A: oral administration with BIC; B: oral administration with BIC-NPs; C: intravenous injection with BIC-NPs.

the pre-treatment of SALLE only diluted the sample twice over and the prepared sample possesses a higher concentration than that in PPT. Consequently, 5 M ammonium acetate was selected as salt for SALLE for sample pre-treatment in this study.

3.4. Method validation

3.4.1. Specificity and selectivity

The MRM chromatograms of blank plasma (A), LLOQ (B), and real plasma sample (C) are shown in Fig. 2. There are no peak observed with the areas higher than 20% of the LLOQ for any analyte, which suggested that the selectivity was considered acceptable.

3.4.2. Residual effects

In the blank sample, no peak with the area of >20% for LLOQ or 5% for IS was detected in each analyte retention time after the ULOQ sample injection. Consequently, the residual effects of this analytical method can be ignored.

3.4.3. Linearity and sensitivity

The hybrid calibration curves, which contained seven concentration points were proved to possess good linearity with a mean coefficient of determination (r) $\geq$ 0.99 over the calibration range

(Table 3). The accuracy of the analytes back-calculated concentration was within the range of 85%–115% with all the verified concentration points.

3.4.4. Precision and accuracy

As shown in Table 4, the accuracy and precision of intra-batch and inter-batch for all analytes in LLOQ and QCs (low, medium, and high) were within the criterion. The value of RR% was between 91.65% and 104.61% and the value of RSD% was between 4.97% and 11.16%. The results suggested that the method was accurate and reproducible. The raw data were supplemented in Table S1.

3.4.5. Extraction recovery and matrix effect

The extraction recovery and matrix effect of all the analytes were determined on the three QC levels and these results are shown in Table 5. The matrix effects of the QC samples ranged from 90.35% to 97.76% (RSD% values <6.65%), and the average extraction recoveries ranged from 87.59% to 102.95% (RSD% values <5.28%). Consequently, the recovery of this method was stable, and the matrix effect could be ignored. The raw data were supplemented in Table S2.

3.4.6. Dilution effect

To demonstrate the dilution integrity of three studied analytes, rat plasma samples were spiked with high concentrations of the three analytes beyond the linear range of the presented method and diluted with blank rat plasma (1:2 and 1:4) then analyzed. As shown in Table S3, the RR% ranged from 91.31% to 103.27 (RSD% was < 8.42%) indicating the integrity of the analytes up to four times dilution of plasma samples.

3.4.7. Stability

The results of RT stability, autosampler stability, freeze–thaw stability, and long-term stability are shown in Table 6. The RR% of RT stability of QC samples ranged from 91.76% to 102.61% (RSD% was < 6.67%). The RR% of injector stability ranged from 91.36% to 100.22% (RSD% was < 8.05%). The RR% of freeze–thaw stability ranged from 91.74% to 104.07% (RSD% was < 8.75%). The RR% of long-term stability ranged from 91.73% to 102.77% (RSD% was < 7.75%). The result suggests that all the bio-samples were stable under the conditions of the existing storage. The raw data were supplemented in Table S4.

3.5. Application of the method to pharmacokinetics study of BIC and BIC-NPs in rats

After an oral doses of 15 mg/kg BIC or BIC-NPs, or an intravenous injection dose of 1.5 mg/kg BIC-NPs, the newly established LC-MS/MS method was performed to determine the concentrations of plasma of the three analytes in rat plasma. The mean plasma concentration–time curves of BIC, the M7, and M8 metabolite in SD rats are displayed in Fig. 3, and the main pharmacokinetic parameters calculated by DAS 2.0, were shown in Table 7 (the raw data were supplemented in Table S5).

BIC was quickly absorbed and metabolized after administration, reaching their maximum concentration (T_{max}) within 0.21 ± 0.08 (h) and with 2.3 ± 0.16 (h) half-life ($t_{1/2}$), which is in good agreement with previous studies(Tan et al., 2008, Tan et al., 2008, Ryu and Yoo 2012, Yang et al., 2019). Compared with BIC, the value of $AUC_{0\rightarrow t}$, $t_{1/2}$, and C_{max} in BIC-NPs were improved to 3.02, 1.43, and 2.37 times, respectively. Meanwhile, the plasma clearance of BIC was reduced from 51.73 ± 23.49 to 12.18 ± 3.36 (L/h/kg), which may contribute to the BIC bioavailability improved (from 8.4% to 25.4%). Interestingly, the $AUC_{0\rightarrow t}$ of M7 were 16.7 times more than that in BIC after administration with BIC. In addition, the C_{max} and $t_{1/2}$ of M7 were 547.54 ± 85.55 (ng/mL) and 3.46 ± 1.48 (h), which

Table 7
The pharmacokinetic parameters of BIC, M7, and M8 in rat after oral administration with BIC or BIC-NPs, or intravenous injection with BIC-NPs (n = 5).

Parameters	ig-BIC			ig-BIC-NPs			iv-BIC-NPs		
	BIC	M7	M8	BIC	M7	M8	BIC	M7	M8
$AUC_{0\to t}$ (ng/mL·h)	383.1 ± 164.4	5627 ± 1261	238.31 ± 52.35	1158 ± 240.5	12415 ± 2467	836.3 ± 264.0	456.1 ± 120.2	434.6 ± 91.9	49.9 ± 21.1
$AUC_{0\to 1}$ (ng/mL·h)	345.3 ± 161.6	9388 ± 8096	359.71 ± 232.72	1322 ± 430.3	15065 ± 4144	1061 ± 187.3	459.3 ± 119.4	463.5 ± 89.1	56.3 ± 19.4
$MRT_{0\to t}$ (ng/mL·h)	3.16 ± 0.77	8.00 ± 0.31	4.62 ± 0.65	3.44 ± 0.60	8.12 ± 0.08	4.89 ± 0.65	0.42 ± 0.31	3.23 ± 0.27	2.11 ± 0.20
$MRT_{0\to 1}$ (ng/mL·h)	4.02 ± 0.79	8.55 ± 0.74	9.42 ± 9.63	3.43 ± 0.53	8.70 ± 0.58	7.19 ± 2.91	0.48 ± 0.33	4.17 ± 0.40	3.64 ± 0.88
$t_{1/2}$ (h)	2.3 ± 0.16	3.46 ± 1.48	5.94 ± 6.56	3.30 ± 1.68	6.12 ± 4.06	5.65 ± 3.54	0.72 ± 0.37	3.68 ± 0.64	3.17 ± 0.57
T_{max} (h)	0.21 ± 0.08	0.8 ± 0.11	1.08 ± 1.34	0.85 ± 0.13	1.1 ± 0.51	2.2 ± 0.83	0.08 ± 0.31	0.15 ± 0.09	0.45 ± 0.11
CLz/F (L/h/kg)	51.73 ± 23.49	5.73 ± 1.44	55.45 ± 23.92	12.18 ± 3.36	2.06 ± 1.22	14.52 ± 2.81			
C_{max} (ng/mL)	119.14 ± 50.66	547.54 ± 85.55	35.79 ± 7.73	283.44 ± 36.35	1042 ± 104.1	121.9 ± 39.0	981.5 ± 143.7	220.7 ± 38.8	40.17 ± 16.90
F_{oral} (%)	8.4 ± 13.7			25.4 ± 20.0					

Note: The data were expressed as mean ± SD; ig.-BIC, administration with BIC; ig.-BIC-NPs, administration with BIC-NPs; iv.-BIC-NPs, intravenous injection with BIC-NPs; $AUC_{0\to\infty}$, area under concentration–time curve from time 0 to infinity; $AUC_{0\to t}$, area under concentration–time curve from time 0 to the last time; Cmax, maximum concentration; T_{max}, peak plasma time; $MRT_{0\to\infty}$, mean residence time under concentration–time curve from time 0 to infinity; $MRT_{0\to t}$, mean residence time under concentration–time curve from time 0 to the last time.

were obviously bigger than that in BIC with 119.14 ± 50.66 (ng/mL) and 2.3 ± 0.16 (h), respectively. Furthermore, the double peak phenomenon was observed on the mean plasma concentration–time curves of M7 after administration with BIC or BIC-NPs, which suggested that the M7 active metabolite may possess the enterohepatic recirculation. It is obviously that both BIC and BIC-NPs were metabolized to abundant M7 active metabolite in SD rat.

4. Conclusion

In conclusion, the main metabolites of optimized BIC-NPs in SD rat plasma were studied and proved to be same with that in BIC. Then, a sensitive and selective LC-MS/MS method to quantify BIC, M7, and M8 in SD rat plasma was developed, validated, and subsequently applied for studying the multicomponent pharmacokinetics of the three analytes after oral administration with BIC or BIC-NPs, or intravenous injection with BIC-NPs. According to the results of the study, the synthetic BIC-NPs was proved to obviously improve the bioavailability of BIC from 8.4% to 25.4% by increasing the plasma concentration and reducing the plasma clearance of BIC. Interestingly, the M7 active metabolite possess enterohepatic recirculation and higher C_{max} and AUC compared with BIC after oral administration with BIC or BIC-NPs, which would provide a basis for researching the treatment mechanism of liver injury. Meanwhile, the metabolism between rat and human was quite different, the similar research will be conducted on human or model group to verify the M7 active metabolite in our future work.

CRediT authorship contribution statement

Xucong Huang: Data curation, Conceptualization, Methodology, Formal analysis, Writing – original draft. **Zhenghua Wu:** Data curation, Conceptualization, Formal analysis. **Yanchao Liu:** Data curation, Conceptualization. **Mengqi Jia:** Data curation, Conceptualization. **Wenjuan Zhao:** Data curation, Conceptualization. **Shuowen Wang:** Data curation, Conceptualization. **Xinhui Jiang:** Writing – review & editing. **Yuefen Lou:** Writing – review & editing. **Guorong Fan:** Project administration, Writing – review & editing.

Declaration of Competing Interest

The authors declare that they have no known competing financial interests or personal relationships that could have appeared to influence the work reported in this paper.

Appendix A. Supplementary material

Supplementary data to this article can be found online at https://doi.org/10.1016/j.arabjc.2023.105287.

References

Ahmed, S., Sparidans, R.W., Lu, J., et al., 2022. A robust, accurate, sensitive LC-MS/MS method to measure indoxyl sulfate, validated for plasma and kidney cells. Biomed. Chromatogr. 36, e5307.

Anthemidis, A.N., Ioannou, K.I., 2009. Recent developments in homogeneous and dispersive liquid-liquid extraction for inorganic elements determination. A review. Talanta 80, 413–421. https://doi.org/10.1016/j.talanta.2009.09.005.

Ferenci, P., 2015. Treatment of hepatitis C in difficult-to-treat patients. Nat. Rev. Gastroenterol. Hepatol. 12, 284–292. https://doi.org/10.1038/nrgastro.2015.53.

Hajkova, K., Jurasek, B., Sykora, D., et al., 2016. Salting-out-assisted liquid-liquid extraction as a suitable approach for determination of methoxetamine in large sets of tissue samples. Anal. Bioanal. Chem. 408, 1171–1181. https://doi.org/10.1007/s00216-015-9221-1.

Huang, X., Jia, M., Liu, Y., et al., 2022. Identification of bicyclol metabolites in rat plasma, urine and feces by UPLC-Q-TOF-MS/MS and evaluation of the efficacy and safety of these metabolites based on network pharmacology and molecular docking combined with toxicity prediction. J. Pharm. Biomed. Anal. 220,. https://doi.org/10.1016/j.jpba.2022.114947 114947.

Huang, X., Wu, Z., Qiaolongbatu, X., et al., 2023. Recycling preparative isolation of six bicyclol active metabolites from SD rat urine using macroporous resin, offline 2D LPLC/HPLC, and prep-HPLC combined with pharmacodynamic evaluation of two active metabolites. Arab. J. Chem. https://doi.org/10.1016/j.arabjc.2023.105107.

Li, M., Wang, H., Huan, X., et al., 2021. Simultaneous LC-MS/MS bioanalysis of alkaloids, terpenoids, and flavonoids in rat plasma through salting-out-assisted liquid-liquid extraction after oral administration of extract from Tetradium ruticarpum and Glycyrrhiza uralensis: a sample preparation strategy to broaden analyte coverage of herbal medicines. Anal. Bioanal. Chem. 413, 5871–5884. https://doi.org/10.1007/s00216-021-03568-1.

Liu, G.T., 2009. Bicyclol: A novel drug for treating chronic viral Hepatitis B and C. Med. Chem. 5, 29–43. https://doi.org/10.2174/157340609787049316.

Liu, Y., Jia, M., Gao, A., et al., 2022. Attenuation of liver injury via bicyclol-bovine serum albumin nanopreparation using a green synthetic approach. J. Nanomater. 2022, 1–11. https://doi.org/10.1155/2022/7740768.

Pavan, M., Yamamoto, P., Moreira da Silva, R., et al., 2022. Chemometric optimization of salting-out assisted liquid-liquid extraction (SALLE) combined with LC-MS/MS for the analysis of carvedilol enantiomers in human plasma: Application to clinical pharmacokinetics. J. Chromatogr. B Analyt. Technol. Biomed. Life Sci. 1205,. https://doi.org/10.1016/j.jchromb.2022.123338 123338.

Rizzo, S., Russo, M., Labra, M., et al., 2020. Determination of chloramphenicol in honey using salting-out assisted liquid-liquid extraction coupled with liquid chromatography-tandem mass spectrometry and validation according to 2002/657 European Commission Decision. Molecules 25. https://doi.org/10.3390/molecules25153481.

Ryu, J.K., Yoo, S.D., 2012. Preparation and evaluation of bicyclol microemulsions for enhanced oral bioavailability. Drug Dev. Ind. Pharm. 38, 1313–1318. https://doi.org/10.3109/03639045.2011.650643.

Tan, W., Wang, B., Zhao, J., et al., 2008. Pharmacokinetics of bicyclol in rats with acute hepatic failure. Xenobiotica 38, 1399–1409. https://doi.org/10.1080/00498250802460733.

Tan, W., Chen, H., Zhao, J., et al., 2008. A study of intestinal absorption of bicyclol in rats: Active efflux transport and metabolism as causes of its poor bioavailability. J. Pharm. Pharm. Sci. 11, 97–105. https://doi.org/10.18433/j3b88v.

Tang, J., Gu, J., Chu, N., et al., 2022. Efficacy and safety of bicyclol for treating patients with idiosyncratic acute drug-induced liver injury: A multicenter, randomized, phase II trial. Liver Int. 42, 1803–1813. https://doi.org/10.1111/liv.15290.

Tang, Y.Q., Weng, N., 2013. Salting-out assisted liquid-liquid extraction for bioanalysis. Bioanalysis 5, 1583–1598. https://doi.org/10.4155/bio.13.117.

Wang, Y., Dellatore, P., Douard, V., et al., 2016. High fat diet enriched with saturated, but not monounsaturated fatty acids adversely affects femur, and both diets increase calcium absorption in older female mice. Nutr. Res. 36, 742–750. https://doi.org/10.1016/j.nutres.2016.03.002.

Yang, S., Hu, J., Li, Y., et al., 2019. Evaluation of pharmacokinetic interactions between bicyclol and co-administered drugs in rat and human liver microsomes in vitro and in rats in vivo. Xenobiotica 49, 987–994. https://doi.org/10.1080/00498254.2018.1524186.

Yao, G.-B., Xu, D.-Z., Lan, P., et al., 2005. Efficacy and safety of bicyclol in treatment of 2 200 chronic viral hepatitis. Zhongguo Xinyao yu Linchuang Zazhi. 24, 421–426.

Yu, H.Y., Wang, B.L., Zhao, J., et al., 2009. Protective effect of bicyclol on tetracycline-induced fatty liver in mice. Toxicology 261, 112–118. https://doi.org/10.1016/j.tox.2009.04.058.

Zhang, J., Wu, H., Kim, E., et al., 2009. Salting-out assisted liquid/liquid extraction with acetonitrile: a new high throughput sample preparation technique for good laboratory practice bioanalysis using liquid chromatography-mass spectrometry. Biomed. Chromatogr. 23, 419–425. https://doi.org/10.1002/bmc.1135.

Zhang, J., Rodila, R., Gage, E., et al., 2010. High-throughput salting-out assisted liquid/liquid extraction with acetonitrile for the simultaneous determination of simvastatin and simvastatin acid in human plasma with liquid chromatography. Anal. Chim. Acta 661, 167–172. https://doi.org/10.1016/j.aca.2009.12.023.

Zhao, J., Chen, H., Li, Y., 2008. Protective effect of bicyclol on acute alcohol-induced liver injury in mice. Eur. J. Pharmacol. 586, 322–331. https://doi.org/10.1016/j.ejphar.2008.02.059.

Zhao, T., Mao, L., Yu, Z., et al., 2021. Therapeutic potential of bicyclol in liver diseases: Lessons from a synthetic drug based on herbal derivative in traditional Chinese medicine. Int. Immunopharmacol. 91,. https://doi.org/10.1016/j.intimp.2020.107308 107308.

Zhao, T.M., Wang, Y., Deng, Y., et al., 2020. Bicyclol attenuates acute liver injury by activating autophagy, anti-oxidative and anti-inflammatory capabilities in mice. Front. Pharmacol. 11,. https://doi.org/10.3389/fphar.2020.00463 463.

Zhen, Y.Z., Li, N.R., He, H.W., et al., 2015. Protective effect of bicyclol against bile duct ligation-induced hepatic fibrosis in rats. World J. Gastroenterol. 21, 7155–7164. https://doi.org/10.3748/wjg.v21.i23.7155.